Squirrel cage induction motor fault diagnosis using lissajous curve of an auxiliary winding voltage: case of broken bars

Jelbaoui Yakout Khadouj[1], El Menzhi Lamiaà[2], Abdallah Saad[3]
[1,2]Departement of Electrical and Industrial Engineering, National School of Applied Sciences,
Abdelmalek Essaadi University, Tangier, Morocco
[3]National Higher School of Electricity and Mechanic, Hassan 2 University, Casablanca, Morocco

Article Info

ABSTRACT

The detection of incipient faults has attracted industrials and researchers specific attention in order to prevent the motor breakdown, improve its reability and increase its lifetime. This paper presents a squirrel cage induction machine broken bar and rings diagnosis approach. This technic uses a new monitored signal as an auxiliary winding voltage related to a small coil inserted between two stator phases. Monitoring behaviors of the Lissajous curve of this auxiliary winding voltage park components under different load levels is the main key of this study. For this purpose, the squirrel cage induction machine modeling and the explicit expressions developed for the inserted winding voltage and its Park components will be presented. Then, an induction machine with different broken cases: one broken bar, two broken bars, broken end ring and broken bars with end ring are investigated. The simulation results confirm the validity of the proposed approach.

Corresponding Author:

Jelbaoui Yakout Khadouj
Departement of Electrical and Industrial Engineering, National School of Applied Sciences
Abdelmalek Essaâdi University, Tangier, Morocco
Email: jelbaoui.yakout@gmail.com

1. INTRODUCTION

The squirrel cage induction motor is the most extensive employed electrical machine in many industrial applications owing to its effectiveness, robustness and its high performance. It present a keystone of electromecanical conversion chain. Thus, any undesired breakdown of the induction machine due to failures is costly. It can lead to stopping production [1]. So, early detection of abnormality is necessary to avoid motor damage. For that purpose, several researchers have continuously been attracted by induction motor fault diagnosis using on-line condition monitoring methods in order to maintain the machines normal operation.

After an induction machine failure surveys, the breakdown occurred in the motor have been categorized according to its main components [2], [3]: stator faults (37%), rotor fault (10%), bearing faults (41%) and others (12%). Even if the rotor faults percentage is only 10%, they represent one of the major [4] fault arising in the squirrel cage induction machine after the openining or shorting stator winding, turn to ground fault and abnormal connection of stator winding. Moreover, the broken bars and rings faults cause several damage in the machines. In early stage, they may not show any symptoms until the fault propagation to the next bars reducing the motor efficiency or provoking a sudden collapse. For that purpose, the early detection and online diagnosis of this kind of failures can be realized by choosing proper signal processor and analyzing the induction machine measurement. This is the key issue for this paper.

A great attention has been devoted to the detection of the squirrel cage induction motor behavior with broken bars and broken end rings. Various condition monitoring approaches have been presented in [5]

that can be classified in three streams [6]: signature extraction-based approaches [6]-[9], model-based approaches and knowledge-based approaches [10]-[13]. The signatude extraction approaches are widly used in on-line monitoring by surveying diffrents signals such as current, voltage, vibration, power and temperature. The motor current signature analysis master of science in customer (MSCA) [14], [15] is included on the extraction approaches. It is powerful in detecting broken bars and end rings and based on spectal analysis method using fast fourier transform [12]-[17] and discrete wavelet transform (DWT) [8], [9].

The auxiliary winding voltage is a new method used for diagnosising the squirrel cage induction machine [18], [19]. It needs the insert of a small coil "sneak" between two stator phases. The main contribution of this paper is to introduce this new technique for diagnosing the squirrel cage induction machine using the lissajous curves of the auxiliary winding voltage park components for detecting various motor faults without disturbing its operation. Then, different cases will be treated in order to show the effectiveness of the proposed method.

After the introduction, modeling the squirrel cage induction machine as a mesh circuit will be presented in section 2. Then, the proposed method will be developed in section 3. In section 4, the simulation results of this technic for broken bars and end rings will be presented.

2. SQUIRREL CAGE INDUCTION MACHINE MODELING

To study squirrel cage induction motor rotor faults, a mesh model of the rotor is required. This mesh takes into account the machine geometric construction. It is constituted of multiple loops consisting of two adjacent rotor bars connected to portions of the end rings. The study is based on the following assumptions [14], [15], [20]: sinusoidally distributed stator windings, infinity iron permeability, neglecting saturation, uniform air gap, neglecting inter-bar currents, evenly distributed rotor bars, and neglecting flux coupling between different winding without air gap crossing.

The motor matrix mathematical model can be written as [18], [21]-[23]:

$$[\,V_s\,] \;=\; [\,R_s\,]\,[\,I_{3s}\,] \;+\; \frac{d\,[\,\phi_{3s}]}{dt} \tag{1}$$

$$\begin{bmatrix} [\,V_r\,] \\ V_e \end{bmatrix} = [\;0\;] = \begin{bmatrix} [R_r] & \frac{R_e}{N_r} \\ \frac{R_e}{N_r} & R_e \end{bmatrix} \begin{bmatrix} [\,I_r\,] \\ i_e \end{bmatrix} + \frac{d}{dt}\begin{bmatrix} [\,\phi_r] \\ \phi_e \end{bmatrix} \tag{2}$$

where [I] is the currents vector, $[R_s]_{3\times3}$ and $[R_r]_{Nr\times Nr}$ are the stator and the rotor resistances matrixes, [V] is the voltage vector. Whereas $[\,L_s\,]_{3\times3}$ is the stator winding inductance matrix, $[\,L_r\,]_{Nr\times Nr}$ is the rotor inductance matrix, $[\,M_{sr}\,]_{3\times Nr}$ is the mutual inductance matrix between stator and rotor. $[\phi_s]$ and $[\,\phi_r]$ are the stator and rotor fluxes vectors respectively. The details of this matrixes are presented in [4], [16]-[18].

Furthermore, the overall mathematical model machine equations can be written as follows:

$$\frac{d\,[\,I\,]}{dt} = -[\,L\,]^{-1}\left([\,R\,] + \frac{d[\,L\,]}{dt}\right)[\,I\,] - [\,L\,]^{-1}[\,V\,] \tag{3}$$

where $\quad [\,I\,] = \begin{bmatrix} [\,I_{dqo}\,] \\ [\,I_r\,] \\ ie \end{bmatrix}$, $[\,V\,] = \begin{bmatrix} [\,V_{dqo}\,] \\ [\,V_r\,] = 0 \\ Ve = 0 \end{bmatrix}$.

The fundamental equation of dynamics lead to determine the mechanical parts of the system, as follow:

$$\begin{cases} J\,\dfrac{d\omega}{dt} = C_{em} - C_r - f_v\omega \\ \qquad \omega = \dfrac{d\theta}{dt} \end{cases} \tag{4}$$

$$C_{em} = \sqrt{\frac{3}{2}}\,p\,L_{sr}\left(I_{qs}\sum_{k=0}^{Nr-1} I_{rk}\cos(Ka) - I_{ds}\sum_{k=0}^{Nr-1} I_{rk}\sin(Ka)\right) \tag{5}$$

where C_{em} is the electromagnetic torque, C_r is the load torque, ω is the mechanical speed and f_v is the friction coefficient. With:

$$L_{sr} = \frac{4\,\mu_0\,N_s\,RL}{e\pi\,p^2}\sin\!\left(\frac{a}{2}\right), \qquad a = \frac{2\pi}{N_r}p \;\; \text{and}\;\; K = 0,\dots,Nr$$

The geometric parameters R, L, and e are defined respectively as the air gap mean radius, the stack length, and the ring thickness.

3. AUXILIARY WINDING VOLTAGE PARK COMPONENTS

As it is known, the inaccessibility of the rotor makes its maintenance and diagnosis difficult to achieve. Therefor, this technic will be extremely beneficial. It was applied previously for a wound rotor induction motor [24], [25]. The method is built considering that a small coil inserted in stator part forming an angle θ_0 with the A stator phase as shown in Figure 1. This auxiliary winding has no conductive contact with other phases but is mutually coupled with all the other circuits either in the stator or in the rotor sides. The main key of this approach is to determine the voltage of this auxiliary winding and its Park components. Monitoring the Lissajous curve of this signal enabls an efficient failures detection.
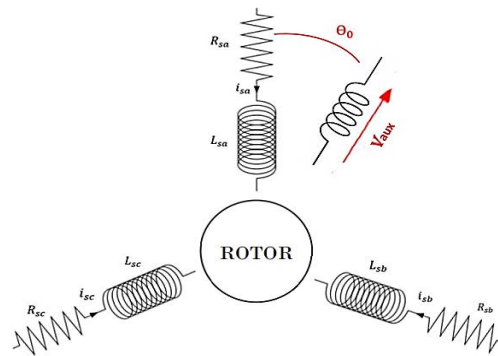
Figure 1. Auxiliary winding emplacement inside the squirrel cage induction motor

Using Runge-Kutta numerical method to resolve the differential matrix (5) we obtain the current vector which allows us to determine the auxiliary winding flux:

$$\varphi_{aux} = a \ I_{sa} + b \ I_{sb} + c \ I_{sc} + \sum_{i=1}^{Nr} d_j \ I_{ri} \tag{6}$$

The coefficients a, b, c and d_j depend on the angle θ_0 such as:

$$a = M_{saux} \ \cos(\theta_0) \qquad\qquad b = M_{saux} \ \cos\left(\frac{2\pi}{3} - \theta_0\right)$$

$$c = M_{saux} \ \cos\left(\frac{4\pi}{3} - \theta_0\right) \qquad\qquad d_j = M_{raux} \cos\left(\theta + \frac{j\pi}{3}\right) \ , \ j = 0,2,4 \ ....$$

M_{saux}, M_{raux} are the stator and rotor with the auxiliary winding mutual inductances respectively.
The auxiliary winding voltage is a function of flux as:

$$V_{aux} = \frac{d \ \varphi_{aux}}{dt} \tag{7}$$

As it is known, the use of Lissajous curve requires the determination of the auxiliary winding voltage Park components. For that purpose, we should consider a three fictive phases system of the inserted coil to which we apply the Park transformation in order to obtain the two components (V_{auxd}, V_{auxq}). Then,

$$V_{auxa} = \frac{d \ \varphi_{auxa}}{dt} \ , \qquad V_{auxb} = \frac{d \ \varphi_{auxb}}{dt} \ , \qquad V_{auxc} = \frac{d \ \varphi_{auxc}}{dt} \tag{8}$$

with,

$$\begin{bmatrix} \varphi_{auxa} \\ \varphi_{auxb} \\ \varphi_{auxc} \end{bmatrix} = [\ A \ ]_{3 \times Nr} \begin{bmatrix} I_{sa} \\ I_{sb} \\ I_{sc} \\ I_{r1} \\ \vdots \\ I_{rNr} \end{bmatrix} \tag{9}$$

Choosing different values of angle θ_0 have no influence on the simulation result. Therefore, we choose θ_0 equal to zero. [A] is the coefficients matrix when $\theta_0 = 0$. Thus φ_{auxa} is represented as:

$$\varphi_{\text{auxa}} = \varphi_{\text{sa}} + \varphi_{\text{sb}} + \varphi_{\text{sc}} + \sum_{i=1}^{Nr} \varphi_{\text{ri}} \tag{10}$$

$$\varphi_{\text{auxa}} = M_{\text{saux}} \; I_{\text{sa}} - \frac{M_{\text{saux}}}{2} \; I_{\text{sb}} - \frac{M_{\text{saux}}}{2} \; I_{\text{sc}} + \sum_{i=1}^{Nr} M_{\text{raux}} \cos\left(\theta + \frac{j\pi}{3}\right) I_{\text{ri}}, \quad j = 0, 2, 4 \dots \tag{11}$$

The flux Park components is defined as:

$$\varphi_{\text{auxad}} = \sqrt{\frac{3}{2}}\left(\varphi_{\text{auxa}} \; \cos(\theta_0) + \varphi_{\text{auxb}} \; \cos\left(\theta_0 - \frac{2\pi}{3}\right) + \varphi_{\text{auxc}} \; \cos\left(\theta_0 - \frac{4\pi}{3}\right)\right) \tag{12}$$

$$\varphi_{\text{auxaq}} = -\sqrt{\frac{3}{2}}\left(\varphi_{\text{auxa}} \; \sin(\theta_0) + \varphi_{\text{auxb}} \; \sin\left(\theta_0 - \frac{2\pi}{3}\right) + \varphi_{\text{auxc}} \; \sin\left(\theta_0 - \frac{4\pi}{3}\right)\right) \tag{13}$$

The expressions of the auxiliary winding voltage Park components are obtained from the derivatives of its flux Park components such as:

$$V_{auxad} = \frac{d\,\varphi_{auxad}}{dt} \qquad and \qquad V_{auxq} = \frac{d\,\varphi_{auxq}}{dt} \tag{14}$$

where,
φ_{auxad} is the direct component of the auxiliary winding flux.
φ_{auxaq} is the indirect component of the auxiliary winding flux.
V_{auxad} is the direct component of the auxiliary winding voltage.
V_{auxaq} is the indirect component of the auxiliary winding voltage.

4.   AUXILIARY WINDING VOLTAGE SIMULATION RESULTS

A broken bar fault is not only limited to the disturbance of the current in the faulty bar, it can give rise to unbalance current in the adjacent bars that increases up to 50% of its value causing breakage of multiple bars. This can lead to a broken end ring and torque pulsation. Moreover, it can generate an excessive vibration in the machine and a louder noise. The stator windings can also be damaged by contacting of the broken bar or its small pieces [9].

The simulations were carried out by MATLAB for a three phase non-defected 450 W squirrel cage motor. The machine parameters values are given in Table 1. Then, this machine was simulated with incipient broken bars and end rings under variable load. To simulate this kind of fault, we increase the bar resistance such as the current of this bar is closest to zero.

During its starting, the machine is healthy. At the time t=1 s the motor is loaded by Cr=1.5 N/m. The failure of the totally broken bar occurs at t=2 s followed by another one at t=3 s. This failure gives rise to oscillations at the speed and the electromagnetic torque curves. The oscillations amplitude, in Figure 2, increases according to the number of the broken bars and their position leading to the speed decreasing in Figure 3.

Table 1. Squirrel cage induction motor parameters

Symbol	Quantity	Value
V	Power supply voltage	220/380 V
f	Frequency	50 Hz
p	Number of pole paires	1
N_r	Number of rotor bars	27
N_s	Number of slots	193
E	Ring thickness	0.38 mm
R	Air gap mean radius	37.5
L	Stack length	60 mm
R_s	Resistanthe stator winding	4.1Ω
R_b	Resistance of a rotor bar	74 μΩ
R_e	Resistance of the rotor end ring	74 μΩ
L_b	Leakage inductance of rotor bars	0.33 μH
L_e	Leakage inductance of rotor end rings	0.33 μH
J	Moment of inertia	$4.5 \; 10^{-3}$ Nms^2

These figures do not give enough informations about faulty motor. Therefore, we apply the method, presented above, based on the Lissajous curve of an auxiliary winding voltage to diagnose the totally broken

bars and end ring failures. The machine is laoded at different levels. The effect of the broken bars in a loaded machine is very noticeable as shown in the figures. The auxiliary winding voltage direct and indirect Park components are used as the diagnostic signal of rotor damages. To validate the proposed approach, a set of simulation is presented for different cases such as: a broken bar, two adjacent broken bars, two separated broken bars, a broken end ring and the compination of two broken bars with an end ring.

In the case of a broken bar, Figure 4 shows the Lissajous curve formed of the auxiliary winding voltage Park components. It has a spiral shape with equally spaced turnings. The pitch of this spiral is substantialy proportional to the load. The more the motor is overloaded, the spiral widens gradually and the pitch changes from about e=10 in Figure 4(a) to e=100 in Figure 4(b).
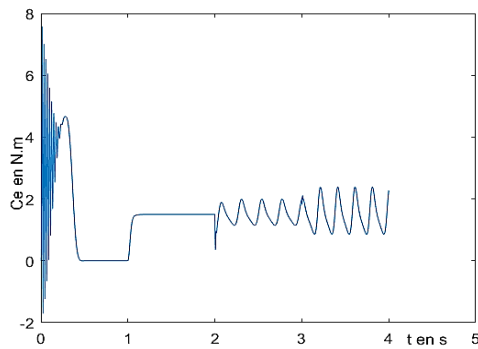
Figure 2. Electromagnetic torque
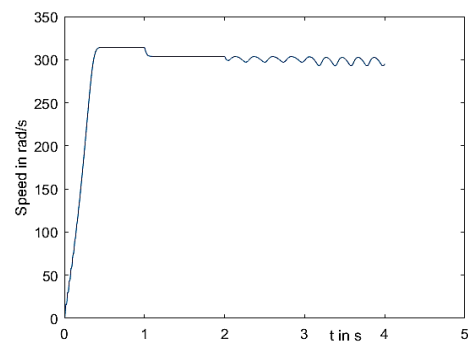
Figure 3. The induction motor speed
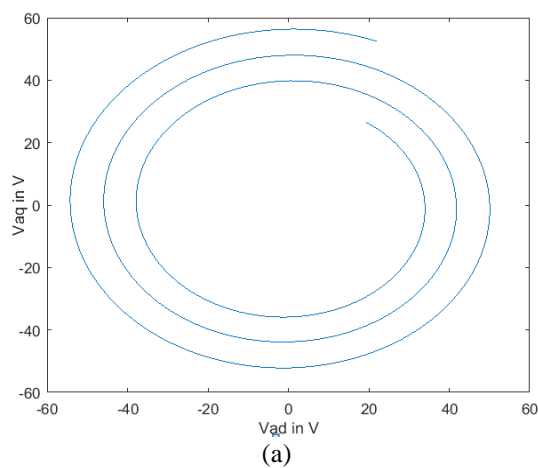
(a)
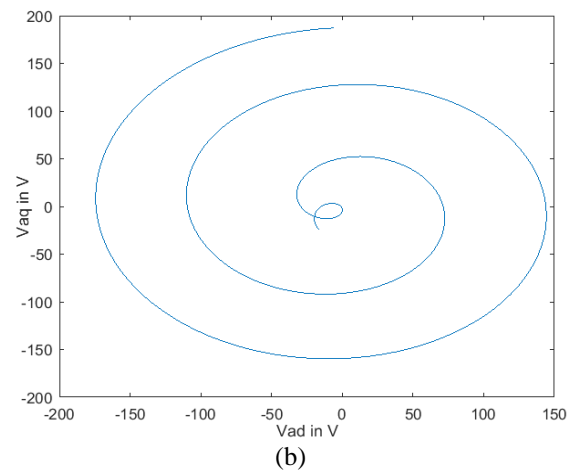
(b)
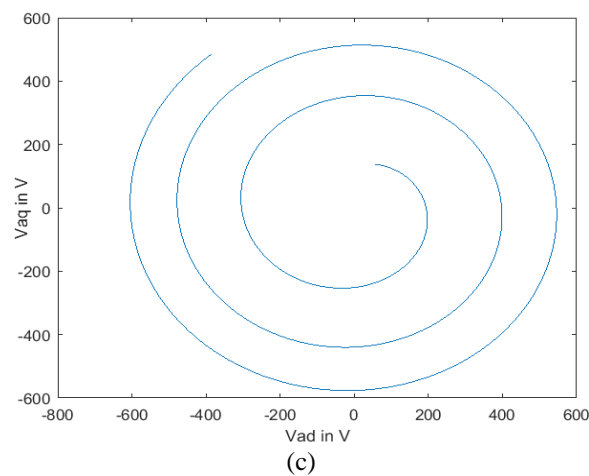
(c)

Figure 4. Lissajous curve of auxiliary winding voltage Park components for one broken bar:
(a) in case of Cr=0.5 Nm, (b) in case of Cr=1.875 Nm and (c) in case of Cr=3 Nm

In the case of two separated broken bars, for a Cr=0.5 Nm, the Lisajous curve has a spiral shape close to a circle with a radius r=145 as shown in Figure 5(a). Once the load increases to Cr=1.875 Nm, the shape of the curve is a clear spiral with a constant separation between the turns e=80 as it appears in Figure 5(b), while at Cr=3 Nm the spiral shape is changed and has lost all its characteristics as shown in Figure 6. For two adjacent broken bars, the simulation results present that the Lissajous curve keeps the spiral shape which continue to widen proportionally with the load as shown in Figure 7. The pitch of the spiral grows gradually with the load and changes from e=9 to e=400.
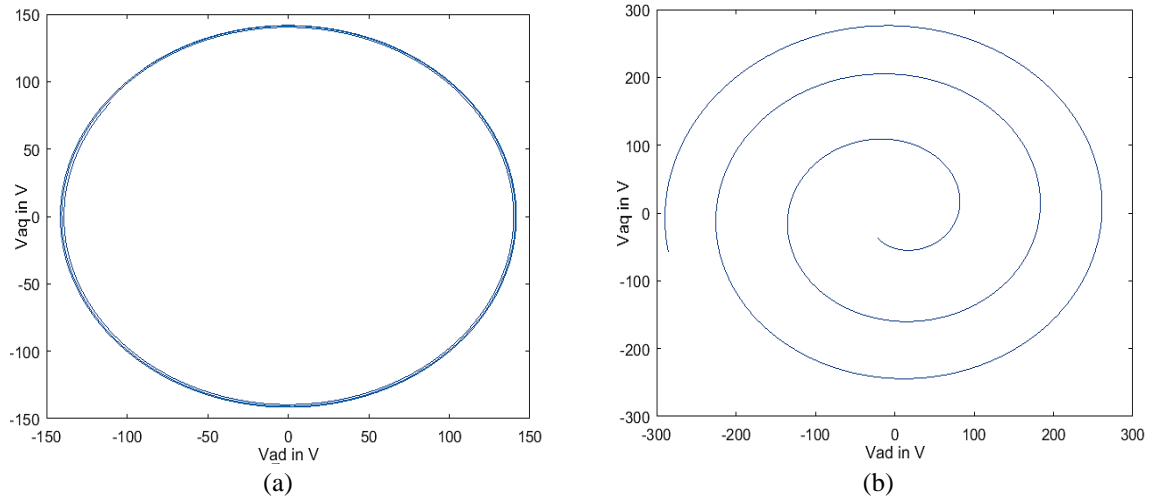
Figure 5. Lissajous curve of auxiliary winding voltage Park components for two separated broken bars:
(a) in case of Cr=0.5 Nm and (b) in case of Cr=1.875 Nm
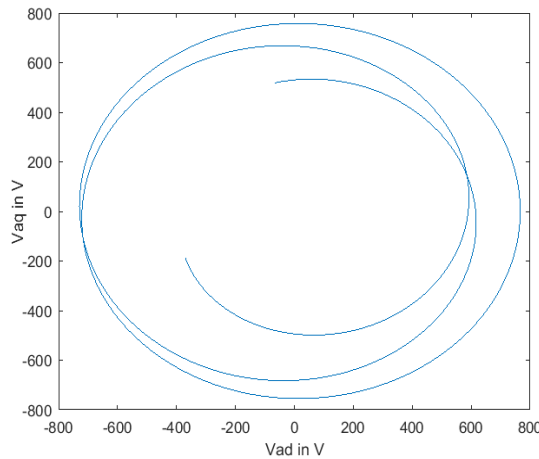
Figure 6. Lissajous curve of auxiliary winding voltage for two separated broken bars with Cr=3 Nm

For a broken end ring rotor shown in Figure 8, the auxiliary winding Park components lissajous curve has the same shape for Cr=0.5 Nm as the one in the case of a broken bar with a different radius r=125 in Figure 8(a). For Cr=1.875 Nm the spiral pitch changes to e=25 Figure 8(b). For Cr=3 N/m, the spiral is more widening until that the pitch reaches e=100 Figure 8(c). The breakage of two adjacent bars leads to a broken end ring. Figure 9 illustrates the simulation result of this combination. The obtained shape is a spiral that also widen with the increasing load. The pitch changed in this case from e=5 for Cr=0.5 Nm to about e=200 for Cr=3 Nm. As far as for Cr=1.875 Nm is concerned, the spires are not equally separated.

(a)

(b)

(c)
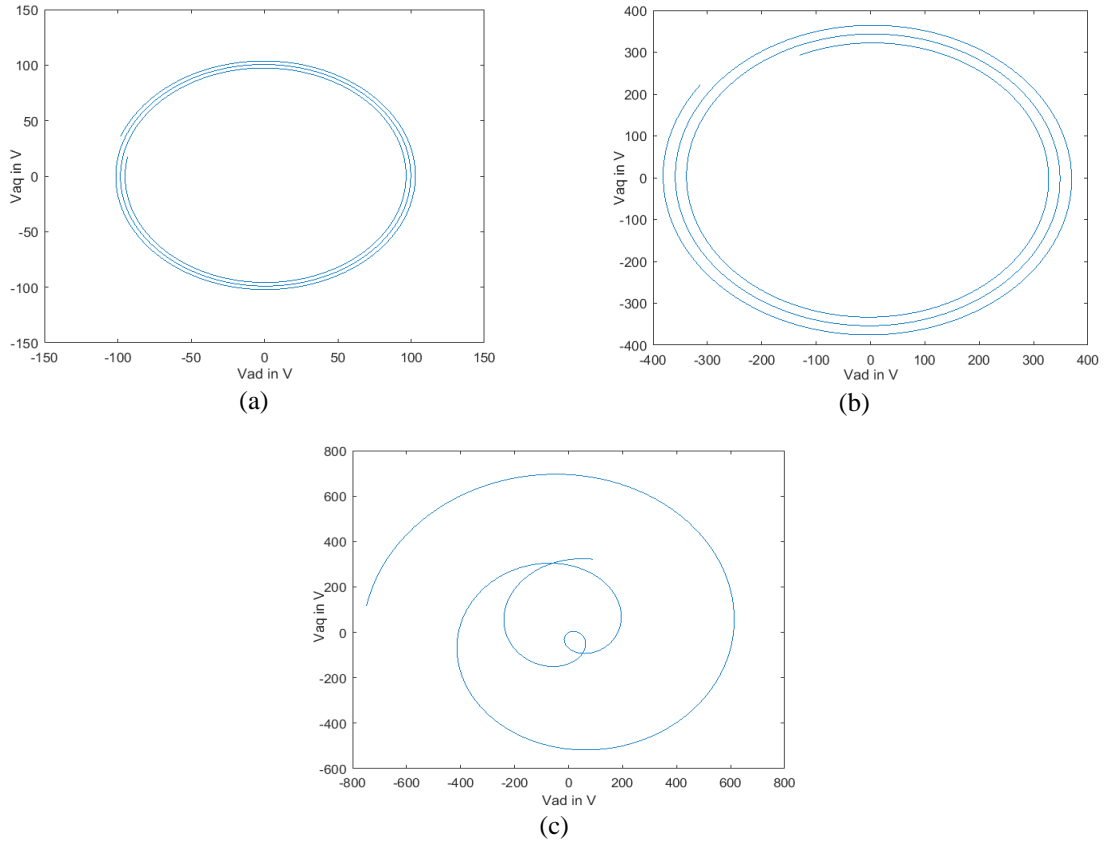
Figure 7. Lissajous curve of auxiliary winding voltage Park components for two adjacent broken bars:
(a) in case of Cr=0.5 Nm, (b) in case of Cr=1.875 Nm, and (c) in case of Cr=3 Nm

(a)

(b)

(c)
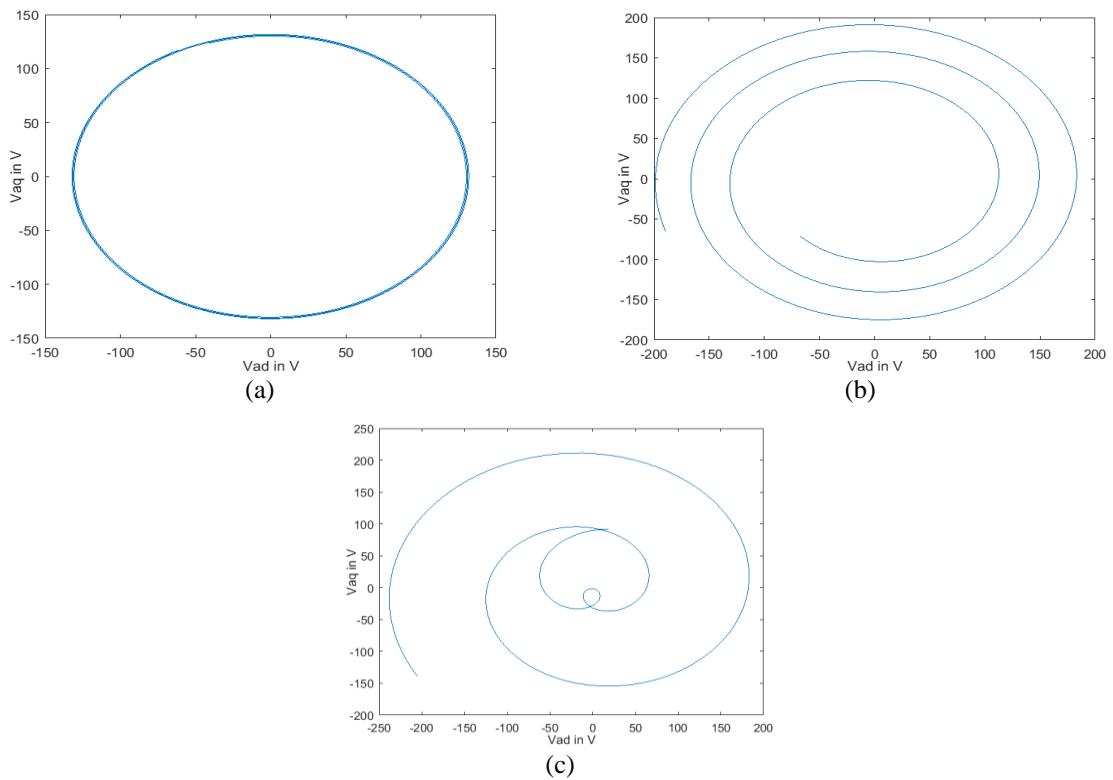
Figure 8. Lissajous curve of auxiliary winding voltage Park components for a broken end ring,
(a) in case of Cr=0.5 Nm, (b) in case of Cr=1.875 Nm, and (c) in case of Cr=3 Nm
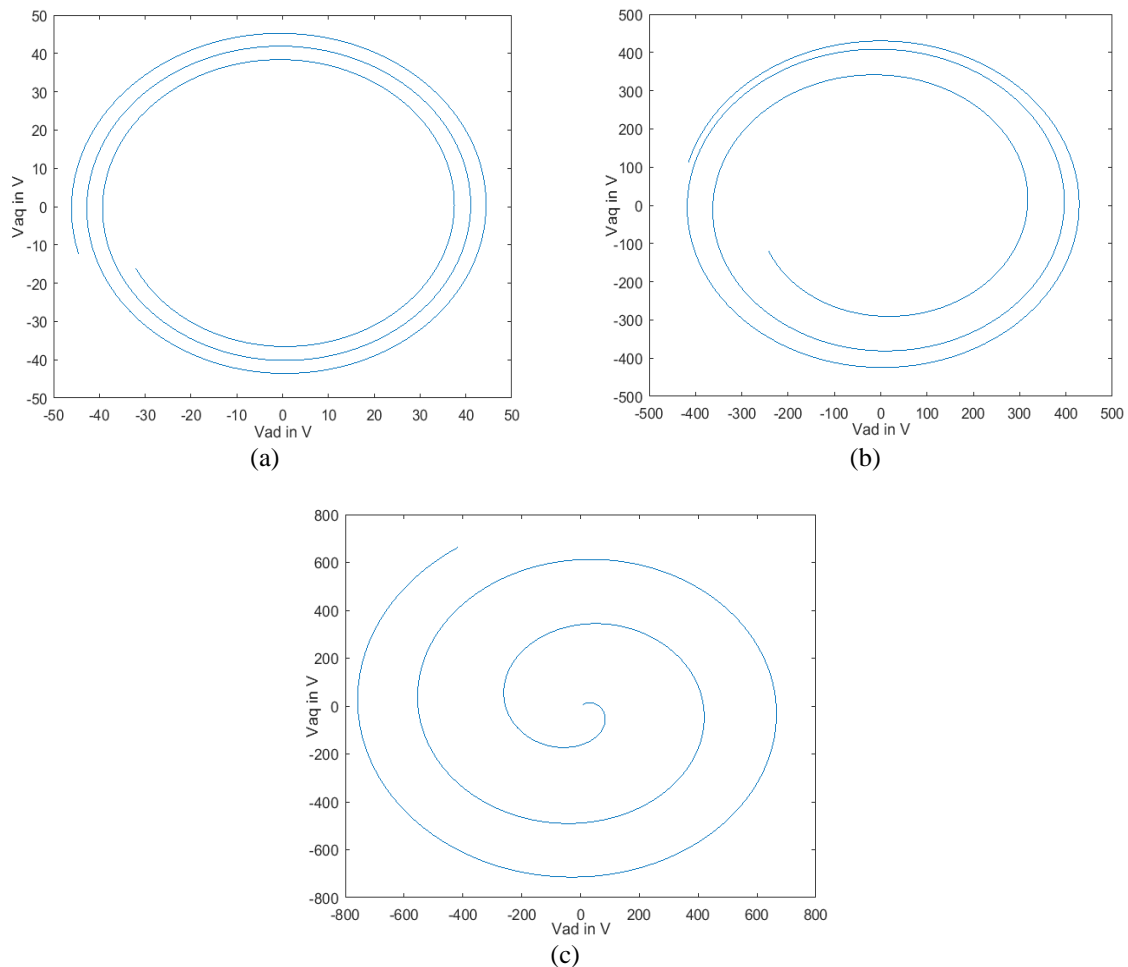
Figure 9. Lissajous curve of auxiliary winding voltage Park components for two adjacent bars and one end ring: (a) in case of Cr=0.5 Nm, (b) in case of Cr=1.875 Nm, and (c) in case of Cr=3 Nm

5. CONCLUSION

A new fault diagnostics technic has been proposed for a squirrel cage induction motor. Based on monitoring the auxiliary winding voltage, the Lissajous curve has been applied to extract informations about the machine state. Simulations were realized on Matlab software for different faults conditions. The results are satisfactory when the machine is loaded at different levels. The shape of Lissajous curve is a spiral that widens proportionally with the motor load. The combination of this diagnosis approach and the auxiliary winding voltage fast fourier transform (FFT) will be presented in a future work in order to study the severity of each failures.

REFERENCES

[1] M. Riera-Guasp, J. A. Antonino-Daviu, and G. A. Capolino, "Advances in electrical machine, power electronic, and drive condition monitoring and fault detection: State of the art," *IEEE Trans. Ind. Electron.*, vol. 62, no. 3, pp. 1746-1759, 2015, doi: 10.1109/TIE.2014.2375853.
[2] J. Y. Khadouj and E. M. Lamiaà, "Electromechanical Conversion Chain Fault Diagnostic - State of Art," *ATS-2018 Proceeding of Engineering and Technology*, vol. 36, pp. 1-5, 2018.
[3] R. Misra, "Condition Monitoring and Fault Diagnosis in Induction Motor : Case Study," *MIT Int. J. Electr. Instrum. Eng.* vol. 5, no. 1, pp. 30-35, 2015.
[4] H. A. Toliyat and T. A. Lip, "of Cage," *Energy*, vol. 10, no. 2, pp. 241-247, 1995.
[5] X. Liang, "Condition monitoring techniques for induction motors," *2017 IEEE Ind. Appl. Soc. Annu. Meet. IAS 2017*, vol. 2017-Janua, pp. 1-10, 2017, doi: 10.1109/IAS.2017.8101860.

[6]   M. Z. Ali, M. N. S. K. Shabbir, X. Liang, Y. Zhang, and T. Hu, "Machine Learning based Fault Diagnosis for Single- and Multi-Faults in Induction Motors Using Measured Stator Currents and Vibration Signals," *IEEE Trans. Ind. Appl.*, vol. 55, no. 3, p. 2378-2391, 2019, doi: 10.1109/TIA.2019.2895797.

[7]   A. Bouzida, O. Touhami, R. Ibtiouen, A. Belouchrani, M. Fadel, and A. Rezzoug, "Fault diagnosis in industrial induction machines through discrete wavelet transform," *IEEE Trans. Ind. Electron.*, vol. 58, no. 9, pp. 4385-4395, 2011, doi: 10.1109/TIE.2010.2095391.

[8]   W. Dehina, M. Boumehraz, and F. Kratz, "Diagnosis of Rotor and Stator Faults by Fast Fourier Transform and Discrete Wavelet in Induction Machine," *2018 Int. Conf. Electr. Sci. Technol. Maghreb*, pp. 1-6, 2018.

[9]   S. Zolfaghari, S. Bahari, M. Noor, and M. R. Mehrjou, "Applied sciences Broken Rotor Bar Fault Detection and Classification Using Wavelet Packet Signature Analysis Based on Fourier Transform and Multi-Layer Perceptron Neural Network,"*Appl. Sci.* vol. 8*,* no. 1, p. 25, 2018, doi: 10.3390/app8010025.

[10]   O. Abdi Monfared, A. Doroudi, and A. Darvishi, "Diagnosis of rotor broken bars faults in squirrel cage induction motor using continuous wavelet transform," *COMPEL - Int. J. Comput. Math. Electr. Electron. Eng.*, vol. 38, no. 1, pp. 167-182, 2019, doi: 10.1108/COMPEL-11-2017-0487.

[11]   X. Liang, S. Member, M. Z. Ali, and S. Member, "Induction Motors Fault Diagnosis Using Finite Element Method : A Review," *IEEE Trans. Ind. Appl.,* vol. 56, no. 2, p. 1205-1217, 2020, doi: 10.1109/TIA.2019.2958908.

[12]   F. Filippetti, G. Franceschini, C. Tassoni, S. Member, and P. Vas, "Recent Developments of Induction Motor Drives Fault Diagnosis Using AI Techniques," *IEEE Trans. Ind. Electron* vol. 47, no. 5, pp. 994-1004, 2000, doi: 10.1109/41.873207.

[13]   Y. Liu, L. Guo, Q. Wang, G. An, M. Guo, and H. Lian, "Application to induction motor faults diagnosis of the amplitude recovery method combined with FFT," *Mech. Syst. Signal Process.*, vol. 24, no. 8, pp. 2961-2971, 2010, doi: 10.1016/j.ymssp.2010.03.008.

[14]   C. Concari, G. Franceschini, C. Tassoni, and S. Member, "Differential Diagnosis Based on Multivariable Monitoring to Assess Induction Machine Rotor Conditions," *IEEE Trans. Ind. Electron* vol. 55, no. 12, pp. 4156-4166, 2008, doi: 10.1109/TIE.2008.2003212.

[15]   T. Deghboudj, A. Derghal, and A. Tlemçani, "Breaking Rotor Bars and Ring Segments Faults on Squirrel Induction Motor: Analytical Study and Comparison of Its Spectral Signatures on Stator Currents," In *International Conference in Artificial Intelligence in Renewable Energetic Systems*, vol 62, 2019, pp. 279-289, doi: 10.1007/978-3-030-04789-4_31.

[16]   J. Seshadrinath, B. Singh, and B. K. Panigrahi, "Vibration Analysis Based Inter - turn Fault Diagnosis in Induction Machines," *IEEE Trans on Ind Inf*, vol. 10, no. 1. pp. 340-350, 2014, doi: 10.1109/TII.2013.2271979.

[17]   A. Menacer, M. d N. T-Said, A. Benakcha, and S. Drid, "Stator Current Analysis of Incipient Fault into Asynchronous Motor Rotor Bars using Fourier Fast Transform," *J. Electr. Eng.*, vol. 55, no. 5, pp. 122-130, 2014, [Online]. Available: http://dspace.univ-biskra.dz:8080/jspui/handle/123456789/2549.

[18]   J. Y. Khadouj, E. M. Lamiaà, and A. Saad, "Diagnosis of a Squirrel cage induction motor Fed by an Inverter Using Lissajous curve of an Auxiliary Winding Voltage," *Ind Journal of Elect Eng and Comp Sci,* vol. 21, no. 3, pp. 1299-1308, 2021, doi: 10.11591/ijeecs.v21.i3.pp1299-1308.

[19]   L. El Menzhi and A. Saad, "Induction motor fault diagnosis using voltage spectrum of auxiliary winding and lissajous curve of its park components," *Adv. Mater. Res.*, vol. 805-806, pp. 963-979, 2013, doi: 10.4028/www.scientific.net/AMR.805-806.963.

[20]   A. Ibrahim and M. Marei, "Modeling of induction motor based on winding function theory to study motor under stator/rotor internal faults," *IEEE proceedings, MEPCON*, no. 1, 2010, pp. 494-500, [Online]. Available: http://www.sdaengineering.com/mepcon10/Papers/215.pdf.

[21]   H. Çaliş and A. Çakir, "Rotor bar fault diagnosis in three phase induction motors by monitoring fluctuations of motor current zero crossing instants," *Electr. Power Syst. Res.*, vol. 77, no. 5-6, pp. 385-392, 2007, doi: 10.1016/j.epsr.2006.03.017.

[22]   M. Boucherma, M. Y. Kaikaa, and A. Khezzar, "Park model of squirrel cage induction machine including space harmonics effects," *Journal of Electrical Engineering*, vol. 57, no. 4, pp. 193-199, 2006.

[23]   M. Ojaghi, M. Sabouria, J. Faizb, and V. Ghorbanianb, "Exact modeling and simulation of saturated induction motors with broken rotor bars fault using winding function approach," *Int. J. Eng. Trans. A Basics*, vol. 27, no. 1, pp. 69-78, 2014, doi: 10.5829/idosi.ije.2014.27.01a.10.

[24]   L. El Menzhi and A. Saad, "Lissajous curve of an auxiliary winding voltage park components for diagnosing multiple open switches faults in three phase inverter," *Appl. Mech. Mater.*, vol. 672-674, pp. 1224-1233, 2014, doi: 10.4028/www.scientific.net/AMM.672-674.1224.

[25]   L. El Menzhi and A. Saad, "Three phase induction motor inverter defects diagnosis using voltage spectrum of an auxiliary winding," *Appl. Mech. Mater.*, vol. 672-674El, pp. 1244-1252, 2014, doi: 10.4028/www.scientific.net/AMM.672-674.1244.

BIOGRAPHIES OF AUTHORS

Yakout Khadouj Jelbaoui was born in Morocco on jully 1992. In 2015, she received the Enginer degree in Mechatronics from the National School of Applied Sciences, Abdelmalek Essaadi University of Morocco in Tetouan. She is PhD student in Electricotechnical engineering at National School of Applied Sciences in Tangier since novembre 2016. She is interested in electrical machines and electrical devices modeling, control and on-line diagnosis defects.

Lamiaa El Menzhi is a professor in AbdelamalekEssaadi University in Morocco since 2010. On 2002, She got her High Deepened Studies Diploma in electrical engineering from the High National School of Electricity and Mechanics ENSEM in Hassan 2 University in Casablanca. From 2002 until 2004, she was a research student in one of the universities in japan. On 2009, she obtained her Doctor degree, then her Habilitation as a professor researcher on 2016 from Hassan 2 University in Casablanca (ESEM). She is interested in electrical machines control and on-line diagnosis either used as a motor or a generator in wind turbines. Lamiaa El Menzhi is a member and advisor of the Moroccan Center of Polytechnical Research and Innovation since 2015.

Abdallah Saad was born in Morocco in September 1956. He received the Engineer and Doctor of Engineering degrees from National Polytechnic Institute of Grenoble France respectively in 1980 and 1982. From 1982 to 1986, he was Researcher at French National Center for Scientific Research (CNRS)-Electrostatics and Dielectric Materials Laboratory Grenoble. After receiving the Doctor of Physical Sciences degree in 1986, he joined Hassan 2 University of Morocco. Professor of electrical engineering, he has several scientific and educational responsibilities. His main fields of interest are High Voltage and Electrical Insulations, modeling and control, renewable energy integration.